



In situ Study of the Function of Bacterioruberin in the Dual-Chromophore Photoreceptor Archaeorhodopsin-4

Chao Sun[†], Xiaoyan Ding[†], Haolin Cui, Yanan Yang, Sijin Chen, Anthony Watts, and Xin Zhao*

Abstract: While certain archaeal ion pumps have been shown to contain two chromophores, retinal and the carotenoid bacterioruberin, the functions of bacterioruberin have not been well explored. To address this research gap, recombinant archaeorhodopsin-4 (aR4), either with retinal only or with both retinal and bacterioruberin chromophores, was successfully expressed together with endogenous lipids in *H. salinarum* L33 and MPK409 respectively. In situ solid-state NMR, supported by molecular spectroscopy and functional assays, revealed for the first time that the retinal thermal equilibrium in the dark-adapted state is modulated by bacterioruberin binding through a cluster of aromatic residues on helix E. Bacterioruberin not only stabilizes the protein trimeric structure but also affects the photocycle kinetics and the ATP formation rate. These new insights may be generalized to other receptors and proteins in which metastable thermal equilibria and functions are perturbed by ligand binding.

Microbial rhodopsins are a class of photoreceptors that share a seven-transmembrane (TM) structure and a light-sensitive retinal (Ret) molecule as the primary chromophore, which is covalently bound to a lysine residue on helix G through a protonated Schiff base linkage.^[1] While they share a similar photoinduced chemical isomerization mechanism, microbial rhodopsins perform diverse functions.^[2] For example, light-driven outward proton and inward chloride pumps create potentials for ATP synthesis, while light-gated ion channels depolarize cells for phototaxis.^[3] Certain photoreceptors contain not only the Ret chromophore but also a noncovalently bound carotenoid molecule as the second chromophore to enable their function. The molecular structure of this carotenoid chromophore varies among photoreceptors. An acyclic C₅₀ carotenoid (bacterioruberin) is present in the crevices between the adjacent subunits within the trimer of archaeorhodopsins (aR), cruxrhodopsins (cR),

deltarhodopsins (dR) and halorhodopsins (hR),^[4] whereas xanthorhodopsin (xR) and Na⁺-translocating rhodopsin (NaR) each contain a cyclized C₄₀ carotenoid (salinixanthin and zeaxanthin, respectively) packed tightly within their protein monomers.^[5]

Archaeorhodopsin-4 (aR4), a proton pump of unknown crystallographic structure found in the claret membrane of *Halobacterium* species (*H. sp.*) XZ515,^[6] is a dual-chromophore photoreceptor with bacterioruberin as the second chromophore, similar to other aRs.^[4a,b] aR4 shares 87% sequence similarity with aR1, 97% with aR2, 84% with aR3, and 59% with bacteriorhodopsin (bR), and exhibits a similar trimeric form with aR2 (Figure 1 a–c).^[7] aR4 employs a similar

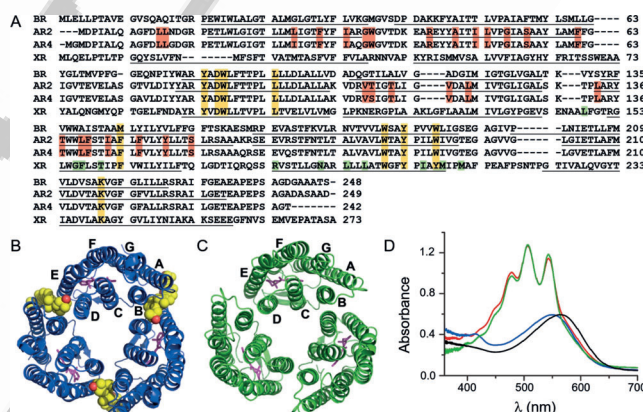


Figure 1. A) Sequence alignment of bR, aR2, aR4, and xR (NCBI No. P02945, P29563, AAG42454 and Q2S2F8, respectively). Red: residues involved in bacterioruberin binding; green: residues involved in salinixanthin binding; orange: residues involved in Ret binding. B and C) Trimeric structure models of aR4 with (B) and without (C) bacterioruberin based on the crystal structures of aR2 (2E14 and 1VGO). Purple: Ret molecule; yellow: bacterioruberin molecule. D) UV/Vis absorption spectra of WT^{XZ515}-aR4 (red), RC^{L33}-aR4 (blue), RC^{MPK409}-aR4 (green), and WT^{R1M1}-bR (black).

light-capture and proton-translocation mechanism to bR, which possesses only a Ret chromophore; however, it displays the opposite temporal order of proton release and uptake to that of bR and aR2 under physiological conditions.^[8] A “weak-coupling model” was proposed to explain the proton transport mechanism of aR4 based on a higher pK_a of the proton-release complex.^[6b] However, the functions of bacterioruberin in aR4 are not well documented, particularly coupling to the Ret binding, photocycle kinetics, and energy conversion. It has been reported that salinixanthin is tightly bound on the TM surface of xR and functions as a light-harvesting antenna.^[9] Its keto ring is buried in a pocket

[*] C. Sun,^[†] Dr. X. Ding,^[†] H. Cui, Y. Yang, S. Chen, Prof. Dr. X. Zhao
Department of Physics, East China Normal University
Shanghai 200062 (P. R. China)
E-mail: xzhao@phy.ecnu.edu.cn

Dr. X. Ding^[†]
Department of Biochemistry and Molecular Biology, Penn State
College of Medicine
Hershey, PA 17033-0850 (USA)
Prof. Dr. A. Watts
Department of Biochemistry, University of Oxford
Oxford OX1 3QU (UK)

[†] These authors contributed equally to this work.

Supporting information and the ORCID identification number(s) for the author(s) of this article can be found under:
<https://doi.org/10.1002/anie.201803195>.

between helices E and F and forms a tight contact with the Ret β -ionone.^[10] However, it is not clear whether a similar specific binding exists between bacterioruberlin and Ret in aR4. The crystal structure of aR2 indicates that bacterioruberlin binds in the crevices between the subunits of the protein trimer, with the polyene chain surrounded by helices A and B of one monomer and helices D and E of an adjacent monomer.^[4b] The residues involved in bacterioruberlin binding in aR2 are quite different from those involved in salinixanthin binding in xR, which are centralized at helices E and F. A question of interest is whether the function of bacterioruberlin in aR4 is the same as in aR2; although all the binding residues in aR2 are identical to those in aR4 (Figure 1A), the temporal orders of proton release and uptake of the two proteins are reversed. In addition, a Ret *cis-trans* isomerization thermal equilibrium commonly occurs in many ion pumps with different molar ratios in the dark-adapted (DA) state and plays an important role in energy conversion.^[11] aR1 has a similar all-*trans* to 13-*cis* molar ratio to that of bR, but this equilibrium largely shifts towards a *trans*-dominated form in aR2.^[12] Whether the presence of bacterioruberlin correlates with the Ret isomerization equilibrium of the archaeal ion pumps has not been documented.

To resolve the issues above, a recombinant aR4 with only the Ret chromophore and endogenous lipids was expressed in *H. salinarum* L33 (denoted by RC^{L33}-aR4). A recombinant aR4 containing both Ret and carotenoid chromophores together with the endogenous lipids was expressed in *H. salinarum* MPK409 (denoted by RC^{MPK409}-aR4). In this way, the functions of bacterioruberlin in aR4 can be investigated in a true in situ manner. Details of the expressions are provided in the Supporting Information. Figure 1D shows the superimposed UV/Vis spectra of WT^{XZ515}-aR4, RC^{L33}-aR4, RC^{MPK409}-aR4, and WT^{R1M1}-bR membranes. RC^{L33}-aR4 shows only a single-peak pattern at approximately 550 nm, similar to the WT^{R1M1}-bR^[13] and the bacterioruberlin-excluded aR4,^[14] thus indicating the presence of only the Ret chromophore in the RC^{L33}-aR4. An identical dominant three-peak pattern at 478 nm, 507 nm, and 543 nm was observed in both WT^{XZ515}-aR4 and RC^{MPK409}-aR4, thus indicating that RC^{MPK409}-aR4 not only contains both Ret and the bacterioruberlin chromophores but also possesses similar bacterioruberlin binding and Ret binding to the wild-type (WT) aR4.^[14] With these two native membrane systems, the functions of the bacterioruberlin in aR4 can be explored systematically.

Patch size and polydispersity indexes obtained by dynamic light scattering (DLS) have been used to determine protein assembly, dimerization, and interactions under various conditions.^[15] A single-peak distribution pattern was observed for WT^{XZ515}-aR4, RC^{L33}-aR4, and RC^{MPK409}-aR4 membranes, with a relatively broader band for RC^{L33}-aR4 (Figure 2A and Table S1 in the Supporting Information). Our results showed that the recombinant RC^{L33}-aR4 and RC^{MPK409}-aR4 had a similar membrane fragment size to WT^{XZ515}-aR4,^[16] thus indicating that the trimeric assemblages of the three proteins are quite similar. However, the polydispersity index of the RC^{L33}-aR4 is twice those of WT^{XZ515}-aR4 and RC^{MPK409}-aR4, thus indicating that the membrane fragment distribution of the RC^{L33}-aR4 is much

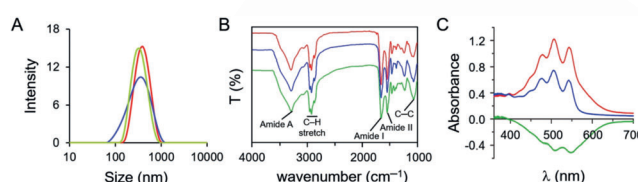


Figure 2. A) Patch-size distributions of WT^{XZ515}-aR4 (red), RC^{L33}-aR4 (blue), and RC^{MPK409}-aR4 (green) membranes. B) FTIR spectra of WT^{XZ515}-aR4 (red), RC^{L33}-aR4 (blue), RC^{MPK409}-aR4 (green). C) UV/Vis absorption spectra of WT^{XZ515}-aR4 before (red) and after (blue) bleaching of the Ret, and the difference spectrum (green).

more dynamic, which may indicate that the packing of aR4 exhibits less rigidity in the absence of bacterioruberlin. Similar sizes and polydispersity indexes were obtained under different protein concentrations. Figure 2B and Figure S7 show the FTIR spectra of WT^{XZ515}-aR4, RC^{L33}-aR4, and RC^{MPK409}-aR4 native membranes. The vibration bands of the amide A and O-H stretching at 3296 cm⁻¹, the C-H stretching at 2959 cm⁻¹, 2929 cm⁻¹ and 2871 cm⁻¹, the amide I stretching of the backbone C=O and C-N bond at 1659 cm⁻¹, and other typical stretching models of the protein are similar in the different proteins (Table S5), thus indicating that the recombinant aR4, with either one or two chromophores, has a similar overall secondary structure to the native form. The C-C stretching at 1548 cm⁻¹ and 1072 cm⁻¹ are also similar. Combining the UV/Vis measurements of WT^{XZ515}-aR4 before and after bleaching of Ret (Figure 2C) and the stability measurements of the three proteins (Table S2), it seems that there is no direct contact between the two chromophores in aR4, which suggests that maintaining the stability of the protein trimer may be the main function of bacterioruberlin, as it is in aR2.^[4b]

A *cis-trans* thermal equilibrium of Ret with different molar ratios in the DA state has been identified in all archaeal proton pumps (Figure 3A).^[12,17] aR1 presents a 50:50 molar ratio for all-*trans* to 13-*cis* in the claret membrane. The recombinant aR3 in *E. coli* membranes also shows a close to 50:50 ratio,^[17] but this molar ratio shifts to 77:23 in aR2.^[12] The difference in this thermal equilibrium may be a result of the substitution of a Ret binding pocket residue at site 146 from Met to Phe in aR2. This argument was supported by the measurement of the Ret thermal equilibrium of the M145F mutant bR.^[4a,12] However, the crystal structures of light-adapted bR and bacterioruberlin-excluded aR2 show a relatively similar Ret binding pocket and Ret polyene chain configuration (Figure S6);^[4a,18] therefore, there may be other unknown factors contributing to this difference.

The Ret thermal equilibrium of aR4 in the DA state was studied for the first time using in situ ssNMR. [10,11,14,15-¹³C₄]-Ret was incorporated into WT^{XZ515}-aR4, RC^{MPK409}-aR4, and RC^{L33}-aR4 membranes using the published methods.^[19] Chemical shift (CS) assignments of Ret at the 10, 11, 14, and 15 sites were obtained through 2D ¹³C-¹³C correlation experiments and 1D double-quantum filtration (DQF) experiments, as shown in Figure 3C-E, Figures S8,9, and Table 1. No large shifts were observed at the 4 sites in either 13-*cis* or all-*trans* forms in these samples. However, +0.7 ppm and -0.3 ppm separation differences of the (C10, C11)_{cis} and (C10, C11)_{trans}

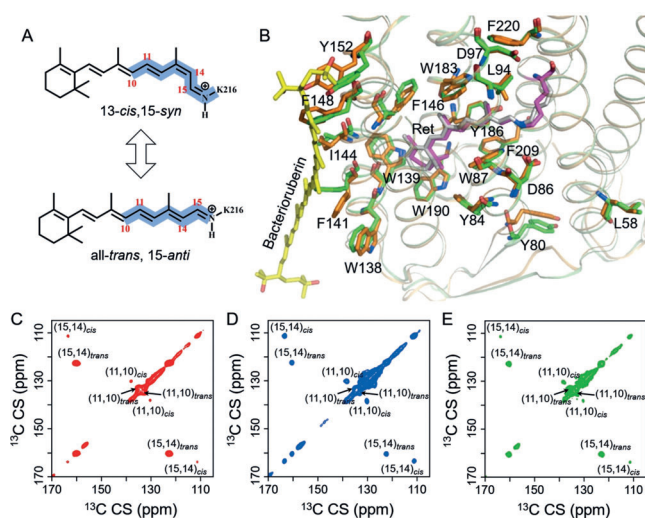


Figure 3. A) Isomerization thermal equilibrium of the Ret chromophore in the DA state. B) Structural comparison of aR2 with (brown) and without (green) bacterioruberin (2E14 and 1VGO). What are these? PDB IDs? C–E) 2D ^{13}C - ^{13}C PDS correlation spectra of [10,11,14,15- $^{13}\text{C}_4$]-Ret-labelled WT^{XZ515}-aR4, RC^{L33}-aR4, and RCMPK409-aR4 in the DA state, respectively.

Table 1: Chemical shifts and the 13-*cis* to all-*trans* isomerization ratios of Ret for WT^{XZ515}-aR4, RC^{L33}-aR4, RC^{MPK409}-aR4, and WT^{R1M1}-bR.^[19]

	13- <i>cis</i>				all- <i>trans</i>				Ratio [%]
	C10	C11	C14	C15	C10	C11	C14	C15	
WT ^{XZ515} -aR4	130.4	138.1	111.5	163.6	133.1	135.0	122.7	160.1	19:81
RC ^{L33} -aR4	130.1	138.5	111.2	163.2	133.2	134.8	122.5	160.3	47:53
RC ^{MPK409} -aR4	130.4	138.2	111.4	163.7	133.1	135.1	122.8	160.2	25:75
WT ^{R1M1} -bR	130.0	139.0	110.0	163.2	133.2	135.4	122.7	160.0	50:50

pairs were observed between RC^{L33}-aR4 and WT^{XZ515}-aR4, and the CS values of Ret in RC^{L33}-aR4 were closer to those in bR. The molar ratios of the two Ret isomers in the DA state were calculated by integration of the (C14 + C15)_{cis} and (C14 + C15)_{trans} peaks through deconvolution and best fitting of the DQF spectra and were verified by CP experiments, as shown in Figure S10,11, Table 1, and Tables S6–10. Various CP mixing times were used to minimize the relaxation effects on the different carbon sites. The molar ratios of the Ret isomers in WT^{XZ515}-aR4 and RC^{MPK409}-aR4 are similar to those in the aR2, with the all-*trans* form dominating.^[12] However, this ratio shifts to a close to equivalent value in RC^{L33}-aR4. It is clear that the shift of the Ret *cis-trans* thermal equilibrium in RC^{L33}-aR4 can be attributed to removal of the second chromophore bacterioruberin. By comparing the crystal structures of aR2 with and without bacterioruberin, it can be concluded that the pumping mechanism could involve bacterioruberin, which is localized at the subunit-subunit boundary, and the absence of bacterioruberin may disrupt interactions among the F141...W138...W139...F146 cluster, thereby resulting in the conformation change of the β -ionone ring of the Ret,^[4a,b] which in turn affects the Ret *cis-trans* thermal equilibrium, as illustrated in Figure 3B. This is the first evidence of a corre-

lation between the Ret thermal equilibrium and bacterioruberin binding. Since the CS of the Schiff base (SB) nitrogen is very sensitive to the Ret configuration, 1D ^{15}N CP experiments were further performed on the ^{15}N -Lys-labelled samples to examine the influence of bacterioruberin (Figure S12). Similar ^{15}N CSs of the backbone nitrogen from the four Lys residues that are at different locations in aR4 were observed in RC^{L33}-aR4 and RC^{MPK409}-aR4, which supports the suggestion that the overall secondary structure of aR4 is still conserved after removal of the bacterioruberin. A -0.8 ppm shift of the SB nitrogen in 13-*cis* isomer and an extra peak at 181.2 ppm, which may represent formation of the L-state as assigned in bR,^[20] were observed in RC^{L33}-aR4. These results indicate that a long-range mediation mechanism between bacterioruberin and Ret may exist and help to modulate the photocycle kinetics of aR4. A greater than 1 nm blueshift for bacterioruberin, and a 28 nm redshift for Ret, as indicated by D86N^{L33}-aR4, in the D86N^{MPK409}-aR4 mutant were observed, thus indicating the existence of such a bidirectional mediation mechanism in this dual-chromophore system (Figure S13).

aR4 shows a proton pumping capability similar to that exhibited by bR but displays an opposite temporal order of proton release and uptake (Figure S14). Photo-isomerization

of the Ret from the all-*trans* to the 13-*cis*, 15-*anti* form triggers a cyclic proton-transfer reaction that includes a series of K-, L-, M-, N-, and O-like photointermediates as in the photocycle of bR.^[3b] The influence of bacterioruberin on the photocycle kinetics of aR4 can be studied based on the light-induced transient absorption change measurements of the M state (410 nm), the O state (660 nm), and the recovery trajectory towards the ground state (570 nm). The complex titration curves of D86 and D97 in the unphotolysed aR4 can also be used to reveal the influence of the protonation status of the proton acceptor D86, the deprotonation kinetics of the protonated SB, and the reprotonation of the proton donor D97 during the photocycle after removal of the second chromophore.^[21] Disturbed photocycle kinetics, particularly a prolonged recovery time towards the initial light-adapted (LA) state, were observed in RC^{L33}-aR4 (Figure 4A and Table S3). A slightly increased pK_a value (0.4 units) for D86 and a slightly decreased pK_a value (0.3 units) for D97 were observed in RC^{L33}-aR4, thus indicating a slightly higher capacity to accept a proton by D86 and a slightly weaker capacity to release a proton by D97 in RC^{L33}-aR4 (Figure 4B–C and Table S4). Perturbation of the photocycle kinetics by the absence of bacterioruberin may be a consequence of an increased pH gradient across the cell membrane, which is generated by the shift of the Ret isomerization thermal equilibrium. This argument was further examined by the measurement of the adenosine triphosphate (ATP) formation rate of the three proteins. *H. salinarum* employs its membrane-bound proton pumping protein to synthesize ATP under anaerobic conditions in the presence of light. The formation of ATP through photophosphorylation generally

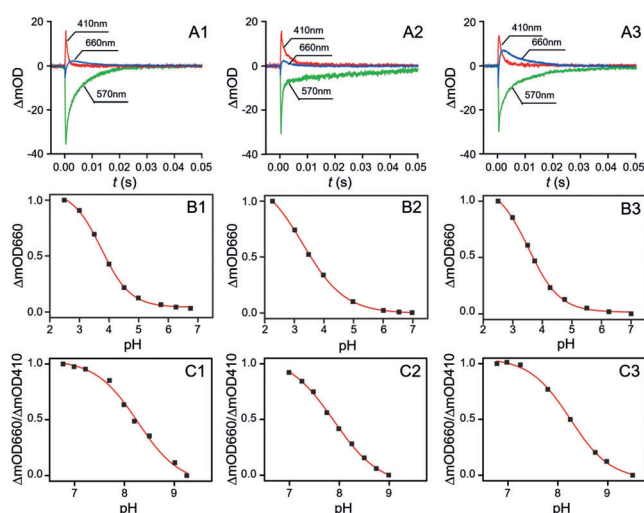


Figure 4. A) Light-induced transient absorption changes in WT^{XZ515}-aR4 (A1), RC^{L33}-aR4 (A2), and RC^{MPK409}-aR4 (A3). B, C) Complex titration curves of D86 and D97 in the claret membranes for WT^{XZ515}-aR4 (B1 and C1), RC^{L33}-aR4 (B2 and C2), and RC^{MPK409}-aR4 (B3 and C3).

has a direct correlation with the proton-pumping capability. Our results showed that the relative ATP formation rate resulting from the photophosphorylation of the aR4 in the MPK409 strains is lower than that of the aR4 in the L33 strains by more than 6% (Figure S15). It has been reported that the highest ATP formation rate is achieved when the light used is closest to the maximum absorption band (550–600 nm) of the Ret chromophore.^[22] This wavelength band corresponds to a 50:50 molar ratio for the Ret isomerization thermal equilibrium.^[23] We found that the molar ratio of Ret is close to 25:75 in both WT^{XZ515}-aR4 and RC^{MPK409}-aR4 and that this molar ratio shifts to 47:53 after removal of the second chromophore in RC^{L33}-aR4. Therefore, the slightly higher ATP formation rate in RC^{L33}-aR4 may be due to its Ret isomerization thermal equilibrium, which is nearer to the optimum. Our suggestion is reasonable since aR4 is a weak proton pump,^[8b] and the modulation by bacterioruberin is suggested to be by indirect moderation. Therefore, the second chromophore bacterioruberin in aR4 may not only affect the trimeric packing dynamics and stability but may also affect the ATP formation rate indirectly by mediating modulation of the Ret isomerization thermal equilibrium of the DA form. Mediation of the Ret isomerization thermal equilibrium by M145F and Y185F mutations in bR has been identified,^[12,19] but no observation has yet been reported for the second chromophore.

In summary, the functional roles of the second chromophore bacterioruberin in aR4 were explored systematically in a true in situ manner. The *cis-trans* thermal equilibrium of the Ret in the DA state shifts to a nearly equivalent form in RC^{L33}-aR4, and is restored to the all-*trans* dominating form in RC^{MPK409}-aR4. A long-range correlation may exist between the two chromophores and play a role in the photocycle kinetics, trimeric structure, and light-energy conversion of aR4. Although other systems such as *E. coli* have been used to express many microbial

rhodopsin proteins with exogenous chromophores, biased Ret isomerization thermal equilibria and protein assembly were obtained in these systems due to the different membrane environments.^[24] The two recombinant aR4 systems provide a unique opportunity for true in situ study of the mediation modulation of the key residues during the photocycle, such as D86, thereby paving the way to more fully explore the proton-pumping and access-switch mechanisms of aR4. These insights might be generalized to other photoreceptors with a dual chromophore.

Acknowledgements

Financial support was provided by the NSFC (30970657, 21475045), SPP (09PJ1404300), and ECNU (79003A29, 79301207, 79301411, 41500-515430-14100) to X.Z. MPK409 strain was a generous gift from Professor Dr. Janos K. Lanyi of University of California, Irvine and Professor Dr. Fang Huang of China University of Petroleum.

Conflict of interest

The authors declare no conflict of interest.

Keywords: chromophores · photoreceptors · protein structures · retinal · structure–activity relationships

- [1] H. Luecke, H. T. Richter, J. K. Lanyi, *Science* **1998**, *280*, 1934–1937.
- [2] a) F. Zhang, J. Vierock, O. Yizhar, L. E. Fenno, S. Tsunoda, A. Kianianmomeni, M. Prigge, A. Berndt, J. Cushman, J. Polle, J. Magnuson, P. Hegemann, K. Deisseroth, *Cell* **2011**, *147*, 1446–1457; b) O. P. Ernst, D. T. Lodowski, M. Elstner, P. Hegemann, L. S. Brown, H. Kandori, *Chem. Rev.* **2014**, *114*, 126–163.
- [3] a) U. Haupts, J. Tittor, D. Oesterhelt, *Annu. Rev. Biophys. Biomol. Struct.* **1999**, *28*, 367–399; b) J. K. Lanyi, *Annu. Rev. Physiol.* **2004**, *66*, 665–688; c) J. M. Walter, D. Greenfield, J. Liphardt, *Curr. Opin. Biotechnol.* **2010**, *21*, 265–270.
- [4] a) N. Enamil, K. Yoshimura, M. Murakami, H. Okumura, K. Hara, T. Kouyama, *J. Mol. Biol.* **2006**, *358*, 675–685; b) K. Yoshimura, T. Kouyama, *J. Mol. Biol.* **2008**, *375*, 1267–1281; c) Q. Li, Y. Zhang, S. Chen, J. Huang, D. Xu, J. Zhang, *Acta Biophys. Sin.* **1993**, *9*, 288–292; d) S. K. Chan, T. Kitajima-Ihara, R. Fujii, T. Gotoh, M. Murakami, K. Ihara, T. Kouyama, *PLoS One* **2014**, *9*, e108362.
- [5] a) Y. V. Bertsova, A. M. Arutyunyan, A. V. Bogachev, *Biochemistry* **2016**, *81*, 414–419; b) S. P. Balashov, E. S. Imasheva, V. A. Boichenko, J. Anton, J. M. Wang, J. K. Lanyi, *Science* **2005**, *309*, 2061–2064.
- [6] a) Q. Li, H. Wang, D. Song, W. Zhao, D. Xu, W. Huang, *Acta Biochem. Biophys. Sin.* **1997**, *29*, 517–520; b) Y. Wang, D. Ma, Y. Zhao, M. Ming, J. Wu, J. Ding, *Acta Polym. Sin.* **2012**, *012*, 698–713.
- [7] L. Tang, Q. a. Sun, Q. Li, Y. Huang, Q. Wei, Y. Zhang, J. Hu, Z. Zhang, M. Li, F. Yang, *Chin. Sci. Bull.* **2001**, *46*, 1897–1900.
- [8] a) E. P. Lukashev, R. Govindjee, M. Kono, T. G. Ebrey, Y. Sugiyama, Y. Mukohata, *Photochem. Photobiol.* **1994**, *60*, 69–

- 75; b) W. Zhao, M. Chai, F. Hai, D. Xu, Q. Li, *Acta Biophys. Sin.* **1998**, *14*, 543–547 ■■■ *Acta Biochem. Biophys. Sin.* ? ■■■.
- [9] S. P. Balashov, E. S. Imasheva, J. M. Wang, J. K. Lanyi, *Biophys. J.* **2008**, *95*, 2402–2414.
- [10] H. Luecke, B. Schobert, J. Stagno, E. S. Imasheva, J. M. Wang, S. P. Balashov, J. K. Lanyi, *Proc. Natl. Acad. Sci. USA* **2008**, *105*, 16561–16565.
- [11] a) X. Ding, Y. Gao, C. Sun, H. Cui, J. Wang, Y. Yang, D. Iuga, F. Tian, A. Watts, X. Zhao, *Biophys. J.* **2017**, *112*, 17a.
- [12] K. Ihara, T. Amemiya, Y. Miyashita, Y. Mukohata, *Biophys. J.* **1994**, *67*, 1187–1191.
- [13] D. Oesterhelt, W. Stoekenius, *Methods Enzymol.* **1974**, *31*, 667.
- [14] Q. Li, Q. Sun, W. Zhao, H. Wang, D. Xu, *Biochim. Biophys. Acta Biomembr.* **2000**, *1466*, 260–266.
- [15] a) E. Ivanova, T. A. Jowitt, H. Lu, *J. Mol. Biol.* **2008**, *375*, 229–239; b) A. Badarau, H. Rouha, S. Malafa, D. T. Logan, M. Hakansson, L. Stulik, I. Dolezilkova, A. Teubenbacher, K. Gross, B. Maierhofer, S. Weber, M. Jagerhofer, D. Hoffman, E. Nagy, *J. Biol. Chem.* **2015**, *290*, 142–156.
- [16] Z. Cao, X. Ding, B. Peng, Y. Zhao, J. Ding, A. Watts, X. Zhao, *Biochim. Biophys. Acta Bioenerg.* **2015**, *1847*, 390–398.
- [17] K. Inoue, T. Tsukamoto, K. Shimono, Y. Suzuki, S. Miyauchi, S. Hayashi, H. Kandori, Y. Sudo, *J. Am. Chem. Soc.* **2015**, *137*, 3291–3299.
- [18] T. Nishikawa, M. Murakami, T. Kouyama, *J. Mol. Biol.* **2005**, *352*, 319–328.
- [19] X. Ding, H. Wang, B. Peng, H. Cui, Y. Gao, D. Iuga, P. J. Judge, G. Li, A. Watts, X. Zhao, *Biochim. Biophys. Acta Bioenerg.* **2016**, *1857*, 1786–1795.
- [20] J. G. G. Hu, B. Q. Q. Sun, A. T. Petkova, R. G. Griffin, J. Herzfeld, *Biochemistry* **1997**, *36*, 9316–9322.
- [21] S. P. Balashov, R. Govindjee, E. S. Imasheva, S. Misra, T. G. Ebrey, Y. Feng, R. K. Crouch, D. R. Menick, *Biochemistry* **1995**, *34*, 8820–8834.
- [22] J. M. Walter, D. Greenfield, C. Bustamante, J. Liphardt, *Proc. Natl. Acad. Sci. USA* **2007**, *104*, 2408–2412.
- [23] M. Tsuda, T. G. Ebrey, *Biophys. J.* **1980**, *30*, 149–157.
- [24] a) J. K. Lanyi, *J. Bioenerg. Biomembr.* **1992**, *24*, 169–179; b) J. W. H. Weijers, S. Schouten, E. C. Hopmans, J. A. J. Geenevasen, O. R. P. David, J. M. Coleman, R. D. Pancost, J. S. Sinninghe Damsté, *Environ. Microbiol.* **2006**, *8*, 648–657.

Manuscript received: March 15, 2018

Accepted manuscript online: May 20, 2018

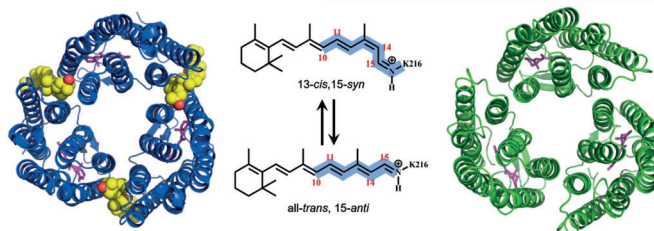
Version of record online: ■■■■■, ■■■■■

Communications

Photoreceptors

C. Sun, X. Ding, H. Cui, Y. Yang, S. Chen,
A. Watts, X. Zhao* ——— ■■■—■■■

In situ Study of the Function of
Bacterioruberin in the Dual-
Chromophore Photoreceptor
Archaerhodopsin-4



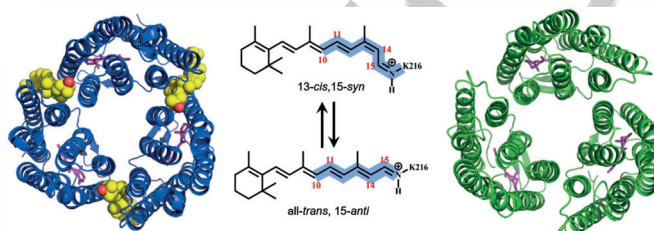
I see your two colors: The carotenoid
chromophore bacterioruberin (yellow)
was found to modulate the *cis-trans*

thermal equilibrium of the retinal chro-
mophore in a dual-chromophore photo-
receptor. ■■■ok? ■■■

Photorezeptoren

C. Sun, X. Ding, H. Cui, Y. Yang, S. Chen,
A. Watts, X. Zhao* ——— ■■■—■■■

In situ Study of the Function of
Bacterioruberin in the Dual-
Chromophore Photoreceptor
Archaerhodopsin-4



Duales System: Der Carotenoidchromo-
phor Bacterioruberin (gelb) moduliert
das thermische *cis-trans*-Gleichgewicht

des Retinalchromophors in einem Pho-
torezeptor mit zwei Chromophoren.

Please check that the ORCID identifiers listed below are correct. We encourage all authors to provide an ORCID identifier for each coauthor. ORCID is a registry that provides researchers with a unique digital identifier. Some funding agencies recommend or even require the inclusion of ORCID IDs in all published articles, and authors should consult their funding agency guidelines for details. Registration is easy and free; for further information, see <http://orcid.org/>.

Chao Sun

Dr. Xiaoyan Ding

Haolin Cui

Yanan Yang

Sijin Chen

Prof. Dr. Anthony Watts

Prof. Dr. Xin Zhao <http://orcid.org/0000-0003-3659-7921>